Available online at www.sciencedirect.com
ScienceDirect
Medical Engineering & Physics 30 (2008) 1089–1097
Medical Engineering & Physics
www.elsevier.com/locate/medengphy

A finite element model to accurately predict real deformations of the breast

A. Pérez del Palomar [a,c,*], B. Calvo [a,c], J. Herrero [b,1], J. López [b,1], M. Doblaré [a,c]

[a] *Group of Structural Mechanics and Materials Modelling, Aragón Institute of Engineering Research (I3A), University of Zaragoza, María de Luna 3, E-50018 Zaragoza, Spain*

[b] *Alma IT Systems, Carolinas 22, E-08012 Barcelona, Spain*

[c] *CIBER on Bioengineering, Biomaterials and Nanomedicine (CIBER-BBN), Aragon Institute of Health (ICS), Spain*

Received 9 January 2007; received in revised form 9 January 2008; accepted 21 January 2008

Abstract

Most surgical procedures in breast plastic surgery are either reconstructive procedures following oncologic interventions (tumorectomy, quadrantectomy, mastectomy . . .) or aesthetic ones, both augmentation and reduction. With current techniques, the results of such procedures cannot be fully guaranteed. Usually, surgical planning is based on a photographic and anthropometric study of the breast only. Among others, one of the difficulties that the plastic surgeons have is the noticeable change of the breast shape with the position of the patient. Thus, it is more and more necessary to plan a presurgical methodology to help the plastic surgeon and guarantee the patient a successful result of the intervention.

In order to establish a reliable simulation method that could predict a patient-specific outcome after breast surgery, this study started trying to correlate spatial features of the breast between lying and standing up positions. A biomechanical model of breast was proposed and implemented into a finite element context to predict deformations, and from these the breast shape in different positions. The resulting shapes were compared with multimodal images, whereas the breast surface displacements were compared with manually identified landmarks and 3D scanner images. From the results, it can be concluded that the model hereby presented reasonably approximates breast response to gravity forces, therefore providing accurate and useful information to the surgeon planning such surgical procedures.

Keywords: Breast biomechanics; Finite element method; Hyperelastic behaviour; Surgery planning

1. Introduction

Plastic surgery has undergone a significant expansion in the last decades with patients obviously demanding accurate and satisfactory outcomes. Medical students and residents who typically learn the surgical procedures by practising on real patients under close supervision, as well as experienced surgeons may find advantage in surgery virtual simulations. They could plan and rehearse complex procedures, predict their outcomes and design and evaluate new methods and equipment. However, the majority of simulation and manipulation systems for surgery have been built using largely phenomenological and heuristic models that have not been validated. This is why modelling the post-surgery deformation of human organs for surgery planning systems has turned out to be a very important subject of research in continuous development.

Regarding breast morphology, this tissue lies on a mobile and irregular muscular bed and is composed of skin, fat and gland which have different mechanical properties that vary according to genetic factors and age [11]. One of the difficulties that plastic surgeons have is the noticeable change of the breast shape with the position of the patient. Moreover, the plastic surgeon performs the surgical procedure with the patient in lying position but needs to move the patient to the standing up position up to five times in order to check the shape of the breast.

Biomechanical breast models mainly employing finite element methods have been explored to predict breast deformations in different situations. Some applications include

* Corresponding author. Tel.: +34 976 76 19 12; fax: +34 976 76 25 78.
E-mail address: amaya@unizar.es (A.P. del Palomar).
[1] Tel.: +34 932 380 592.

1350-4533/$ – see front matter © 2008 IPEM. Published by Elsevier Ltd. All rights reserved.
doi:10.1016/j.medengphy.2008.01.005

guiding clinical biopsy [1], modelling compressions similar to X-ray mammography [12], registering X-ray and MR mammography, validating non-rigid registration algorithms [15], and testing reconstruction algorithms for elastography [17]. The use of mechanical models in these applications is responsible for providing information about the expected deformations. This prior information helps to constrain possible solutions and thus provides a physical basis for interpolation, reconstruction and prediction for those cases in which there is insufficient information in the image data. These biomechanical breast models have been assessed based on the predicted location of anatomical landmarks selected in breast images acquired before and after in vivo compression by visual comparison of the simulated compressed breast image with the uncompressed breast [1]. However, the small number of landmarks available in a single dataset makes these evaluations limited.

A wide range of values for the material properties of the different tissue types involved has been used in the previously cited papers. The constitutive material parameters for fibroglandular and fatty tissues are generally obtained from ex vivo indentation tests [4]. Azar et al. [1,2], Wellman et al. [18] and Krouskop et al. [7] assumed exponential, Samani et al. [13] hyperelastic and Krouskop and Bakic [4] linear elastic stress–strain relationships and used different material parameters. Samani used a hyperelastic material model to approximate Wellman's stress–strain properties. Azar [1–3] applied the same material model as Wellman, but used a corrected stress–strain relationship for fat tissue. All authors considered quasi-incompressible materials with a Poisson ratio close to 0.5. Ruiter et al. [12] concluded that the results do not vary within a significant range of stiffness ratios of gland and fat regarding the required simulation accuracy. The exponential and Neo–Hookean models can be used as approximations, whereas the linear elastic approaches do not perform that well. They argued that the simplest tissue model for breast simulation was the Neo–Hookean one, ignoring the differences between the material properties of gland and fat. With regard to the skin, Samami et al. [13] made the assumption that it can be considered as linear elastic and isotropic for strains lower than 50%. Reihsner et al. [9] examined the two-dimensional mechanical behaviour of human skin samples obtained from different anatomical sites, noting that skin had varying degrees of anisotropy in different regions of the body. By comparing different biomechanical breast models Tanner et al. [16] found that, for a compression of 20%, the effect on accuracy caused by the modification of the material properties was however less significant than the application of correct boundary conditions. Using the displacements of the surface of the breast as boundary conditions, they were able to recover the displacement of validation landmarks to a mean error of less than 2.5 mm.

The aim of this study was to determine a suitable approach to construct breast models that can be employed for simulating plausible breast deformations at different stages. In this paper, we present a virtual deformable breast model whose geometry is constructed from CT images on lying prone position. The image sets were used to reconstruct the contour of the breast without distinguishing fatty and fibroglandular tissue in the volumetric representation. In this work, it was hypothesized that the structural complexity of the breast can be simplified by only assigning an average value of mechanical properties to the glandular and fatty tissue into the 3D image volume. The effect of the gravity force was evaluated. The breast surface displacements were compared with manually identified point landmarks and 3D scanner images in a standing position.

2. Materials and methods

Two data sets corresponding to two women were processed. The first patient (Patient A), a 52 years old female potential recipient of breast reduction, presented a high proportion of fat respect to gland tissue; the second one (Patient B), a 36 years old female potential recipient of breast augmentation, presented a lower proportion of fat respect to gland tissue. The geometry of both models was constructed using CT images of the patients lying horizontally. From the DICOM images, each volumetric model was constructed using voxels, adding the information regarding the density of each material (defined in Hounsfield units) (Fig. 1). Then, a surface mesh with triangles (STL) was created for each of the tissues (gland, fat, muscle and bone). These meshes were constructed applying a Marching Cube algorithm using maximum and minimum threshold densities for each tissue. Once the models were constructed, the bones and muscles were removed obtaining the models shown in Fig. 2.

The volume associated with both STL models was meshed automatically in Harpoon v.2 using tetrahedral elements. Since the accuracy of tetrahedral elements is related to mesh density, a fine enough mesh was made to minimize numerical errors. To define the skin, a surface coating of the solid volume was performed. This surface was meshed using membrane elements with uniform thickness and a full contact was assumed between skin and the remaining tissues.

The distinction between glandular and fat tissues, although possible, was neglected by assigning them an average value of the mechanical properties for the whole breast tissue depending on the estimated percentage of each tissue (see Fig. 3). The estimation was made based on the volume of each tissue measured in the segmentation procedure. Patient A had an estimated 90/10 fat/gland proportion whereas Patient B had an estimated 60/40 proportion.

As mentioned before, there is significant variation in the material properties used to simulate breast deformation. Table 1 depicts the range of variation of the material properties of the different tissues involved using different constitutive models reported in the literature.

One of the main goals of this work was to characterize in the simplest way possible the behaviour of the tissues involved in the breast using the deformation of the breast

Fig. 1. Segmentation of the breast distinguishing the different tissues (Patient A).

between two different positions. Once this behaviour is determined and is valid for achieving the deformation of another known deformed breast, this material model could be used to predict the deformation of any breast knowing only the proportion of each tissue. In this work, these material properties were fitted using the information of the deformed breast from the reference position (patient in lying prone position) and the final position (patient in standing position). Fitting of the material properties of the tissues involved, was accomplished from a finite element model developed from CT images of the patient in vaulted position, simulating first that the breast is without gravity. Then the patient is moved to a vertical position with the gravity (Fig. 4) as it is in standing up position. The adipose and fibroglandular tissues were assumed to be isotropic hyperelastic and quasi-incompressible, and the corresponding parameters were obtained by fitting experimental data to the simplest hyperelastic model, that is the Neo–Hookean model. A user material subroutine was implemented in ABAQUS v.6.5 [6]. Locking of the tetrahedral elements was avoided by using a standard mixed theory.

In this material subroutine, a strain energy density function for quasi-incompressible hyperelastic materials in terms of the strain invariants was introduced. Based on the kinematic assumption, the free energy function was written in the

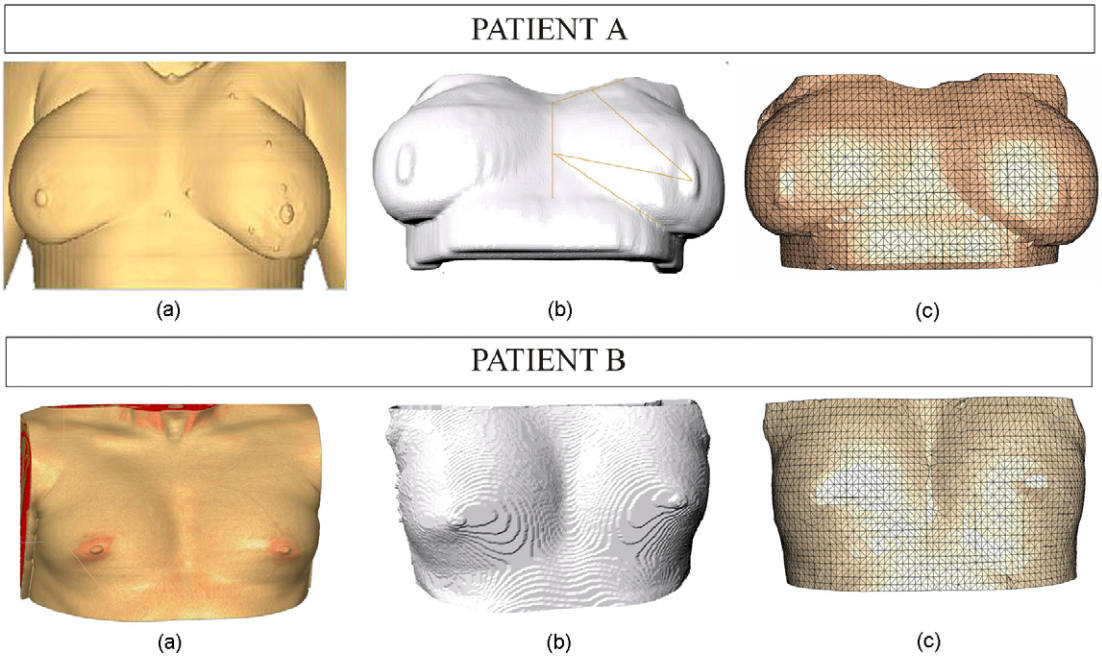

Fig. 2. Geometry reconstruction and finite element mesh of both patients A and B; (a) CT data, (b) surface mesh with triangles (STL), (c) finite element mesh (FEM).

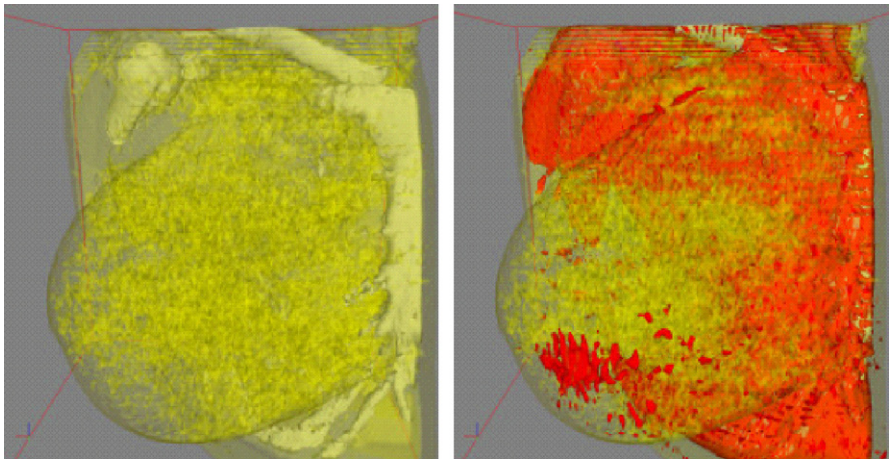

Fig. 3. Segmentation data of Patient A. Fat tissue is shown in yellow, and glandular and muscular tissues are plotted in red. (For interpretation of the references to colour in this figure legend, the reader is referred to the web version of the article.)

Table 1
Material constants for different strain energy density functions proposed by several authors for fat and fibroglandular tissue, E corresponds to the Young modulus in elastic models, C_1 is the constant to define the Neo–Hookean model $\psi = C_1(I_1 - 3)$, constants C_{10}, C_{01}, C_{11}, C_{20}, C_{02} define the polynomial model $\psi = \sum_{i+j=1}^{N} C_{ij}(I_1 - 3)^i(I_2 - 3)^j$ and constants b and m define an exponential model for the Young modulus $E_n = b_n e^{m_n \varepsilon_n}$

Reference	Constitutive model	Fat	Fibroglandular
Tanner et al. [16]	Elastic	$E = 1$ kPa	$E = 1{:}20$ kPa
	Neo–Hookean	$C_1 = 0.13{:}3.5$ kPa	$C_1 = 0.13{:}105$ kPa
		$C_{10} = 46.4 \pm 10$ kPa	$C_{10} = 26.07{:}263.1$ kPa
		$C_{01} = -31.7 \pm 7$ kPa	$C_{01} = -15.56{:}{-}231.32$ kPa
	Polynomial	$C_{11} = 1.96 \pm 0.64$ kPa	$C_{11} = 1.71{:}55.81$ kPa
		$C_{20} = 37 \pm 3.1$ kPa	$C_{20} = 8.1{:}387.5$ kPa
		$C_{02} = 0.08 \pm 2$ kPa	$C_{02} = -0.02{:}0.52$ kPa
Azar et al. [1]	Exponential	$b = 4460$ Pa; $m = 10$	$b = 15{,}100$ Pa; $m = 10$
Roose et al. [10]	Elastic	$E = 1.7{:}500$ kPa	$E = 1.7{:}500$ kPa
Samani et al. [14]		$C_{10} = 0.31 \pm 0.03$ kPa	$C_{10} = 0.33 \pm 0.04$ kPa
		$C_{01} = 0.3 \pm 0.02$ kPa	$C_{01} = 0.28 \pm 0.03$ kPa
	Polynomial	$C_{11} = 2.25 \pm 0.3$ kPa	$C_{11} = 4.49 \pm 0.8$ kPa
		$C_{20} = 3.8 \pm 0.6$ kPa	$C_{20} = 7.7 \pm 1.1$ kPa
		$C_{02} = 4.7 \pm 0.7$ kPa	$C_{02} = 9.45 \pm 1.3$ kPa

decoupled form as

$$\psi(\mathbf{C}) = \psi_{\text{vol}}(J) + \psi_{\text{iso}}(\mathbf{C}^{\text{s}}) = \frac{1}{D} + C_1(I_1 - 3) \tag{1}$$

where $\psi_{\text{vol}}(J)$ and $\psi_{\text{iso}}(\mathbf{C}^{\mathbf{s}})$ are given scalar-valued functions of $J = \det \mathbf{F}$, $\mathbf{C}^{\text{s}} = J^{2/3}\mathbf{F}^{\mathbf{T}}\mathbf{F}$, which describe the volumetric (or dilational) and the isochoric (or distortional) responses of the material, respectively being $\mathbf{F}$ the deformation gradient. As mentioned before, in this work a Neo–Hookean function was used for ψ_{iso}.

Regarding the skin, even though this tissue is anisotropic, its behaviour was approximated by a hyperelastic model able to withstand large deformations [1]. A polynomial strain energy density function was fitted to the experimental results

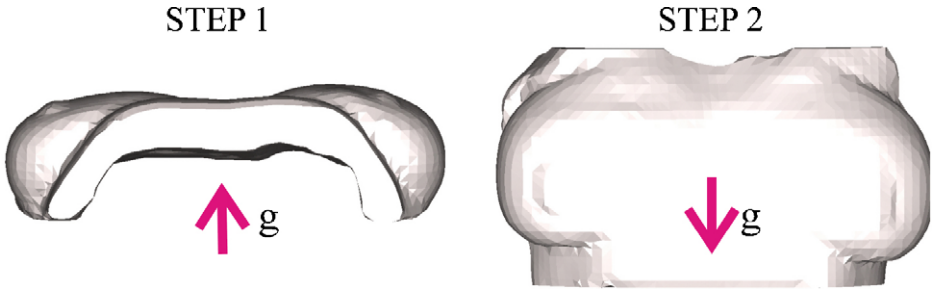

Fig. 4. Loading scheme. First step: the effect of the gravity in prone position is compensated in order to have a model "without gravity". Second step: the gravity load is simulated in order to reproduce the position of the patient in standing up position.

obtained by Gambarotta et al. [5]. The material parameters obtained were: $C_{10} = 31$ Pa, $C_{01} = 30$ Pa, $C_{11} = 22.5$ Pa, $C_{20} = 50$ Pa and $C_{02} = 60$ Pa, and a thickness of 1.0 mm [1] was considered. The chest wall was assumed to fully restrain displacements.

3. Results

Two patients were analyzed to adjust the mechanical properties and to validate the proposed model. First, a woman with a high proportion of fat tissue (Patient A) was analyzed and the material constants were fitted using as reference the motion of several landmarks located on the patient. In second place, these material constants were used for the characterization of the deformation of the breast of a second patient (Patient B) with a different proportion of fat/fibroglandular tissue, and the final shape of the breast was compared with 3D images of the patient in standing position.

3.1. Patient A

In Fig. 5, the positions of different characteristic points drawn by the plastic surgeon are shown. It can be seen how the distances between these points changed when the patient moves from the lying to the standing position. These points were located also in the finite element model by using small titanium balls during the CT acquisition and therefore the new location of these markers in the deformed breast after loading could be compared with the actual locations on the patient.

The proportion of each tissue gland/fat was estimated from the segmented images. For this patient, it was estimated that only the 10% of the total volume was formed by fibroglandular tissue. With this estimation, the mechanical properties were introduced averaging the stiffness of the fat and glandular tissues by weighting the proportion of each component. An iterative procedure varying the material properties was performed until achieving the correct position of the landmarks in the deformed configuration. Fig. 6 shows the position of the markers in the undeformed mesh (patient lying in the CT platform) and after the simulation (patient in standing position). As in the actual patient (Fig. 5) the distances between the landmarks were measured and therefore the material constants were iteratively adjusted to minimize the error between the experimental measurements and the displacement predictions.

In the first run, an average value of C_1 of 2.5 kPa was assigned. The quality of fit of this parameter was evaluated based on an objective or cost function which compares the

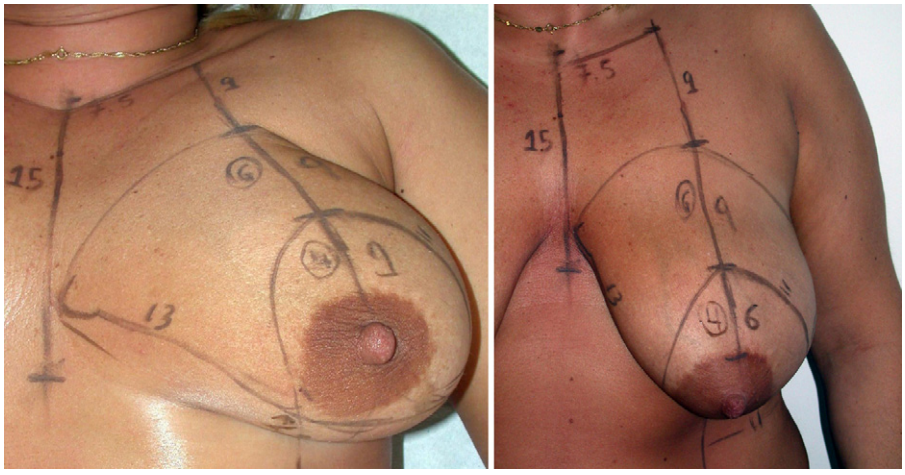

Fig. 5. Anthropometric measures of Patient A. The distances between the reference points vary with the position.

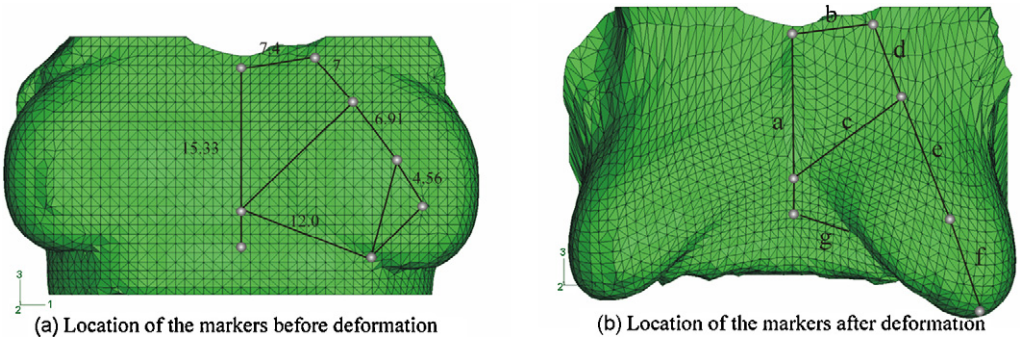

Fig. 6. Location of the markers before and after gravity simulation. Data corresponding to Patient A.

measured data and the FE analysis predicted solution. The objective function o_j, was defined in terms of the sum of the squared residuals between the experimental and predicted results

$$o_j = \sum_{i=1}^{N_d} (D_i^{FE} - D_i^{exp})^2 \quad (2)$$

where o is the cost function, j is the iteration number and superscripts "FE" and "EXP" represent finite element analysis and experimental results, respectively.

The running process was stopped when the objective function satisfied the following criterion:

$$|o_{j+1} - o_j| \leq \Delta$$

being Δ a prescribed specific limit value for the convergence [12].

The final value of C converged to 3.9 kPa which according to the volume fraction law (90% fat/10% gland) means a value of 3 kPa for the fat and 12 kPa for the gland. The comparison of the distances between markers for the actual patient and the virtual model with this value is shown in Table 2.

Table 2
Distances (in cm) between the markers with $C = 3.9$ kPa (Poisson's ratio 0.499)

	a	b	c	d	e	f	g
Patient (lying)	15	7.5	–	4.6	6	4	13
Patient (standing up)	15	7.5	–	7	9	6	13
$C = 3.9$ kPa	15.8	7.6	–	7.5	9.6	6.3	12.2
Error (%)	5.7	1.5	–	7.1	6.7	5	6.1

Comparison with real distances measured on Patient A.

3.2. Patient B

Once the model was adjusted for Patient A, the same material properties were used for the other patient in order to see if these properties were applicable. The morphology of this breast was completely different, and the procedure of validation was also different. The reconstruction of the model was similar to the previous case, but the validation was in this case made using the digitalized image reconstructed from a 3D scanner. This reconstruction was made by merging different photos captured from different angles for Patient B in standing position. Several reference points were located on the patient, in order to get and accurate merge. The mapping of these images was performed and the final reconstruction of the patient can be seen in Fig. 7. This surface was exported in vrml format and was compared with the final shape of the breast after simulation.

Using the same material properties as in Patient A but with a different volume ratio of each constituent, the simulation of moving the patient from the lying position to the standing up position was performed. The volume ratio of each tissue (gland/fat) was computed as in Patient A using the segmentation. The relevance of introducing the correct relation between fat and gland can be seen qualitatively in Fig. 8. In this figure the real 3D image of the

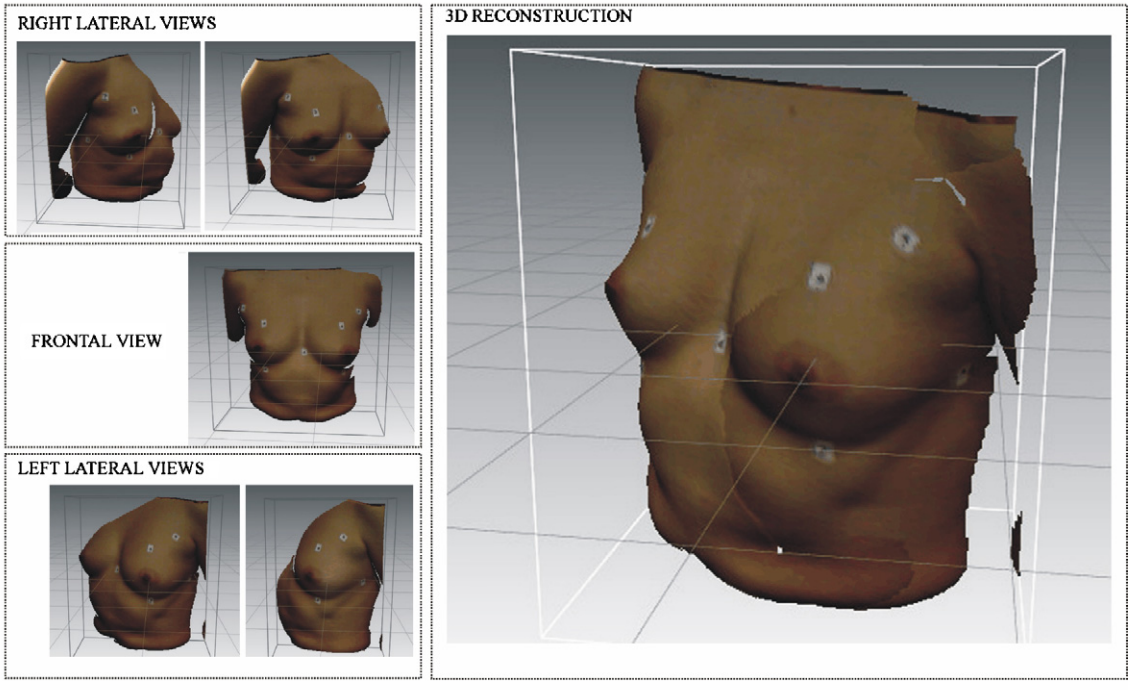

Fig. 7. 3D scanner data. On the left, sequence of images of the patient from different points of view; on the right 3D reconstruction of Patient B in standing up position.

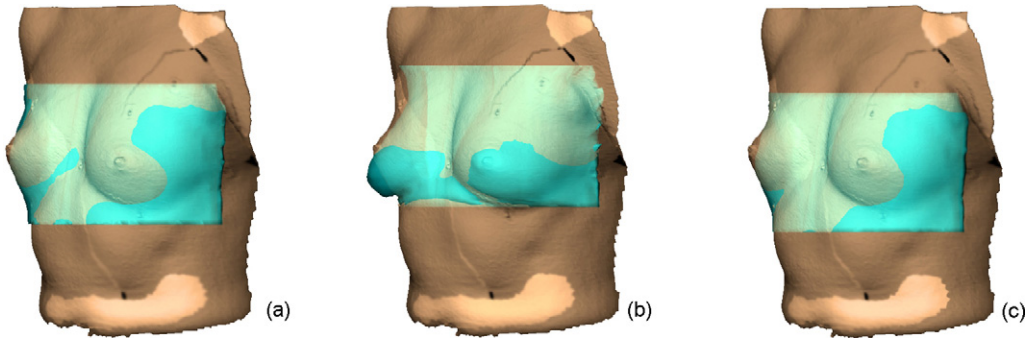

Fig. 8. Superposition of images. The flesh coloured image corresponds to the reconstruction with the 3D scanner and the blue one with the deformed finite element mesh after simulation. (a) 40% fat, 60% gland; (b) 80% fat, 20% gland; (c) 50% fat, 50% gland. (For interpretation of the references to colour in this figure legend, the reader is referred to the web version of the article.)

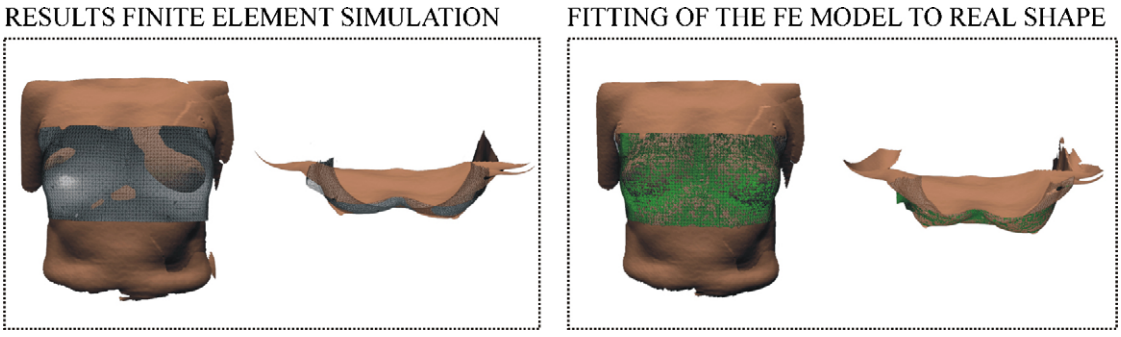

Fig. 9. On the left superposition of the finite element results and the 3D reconstruction of Patient B. On the right the deformed mesh after adjusting it to the real shape of the patient in standing up position.

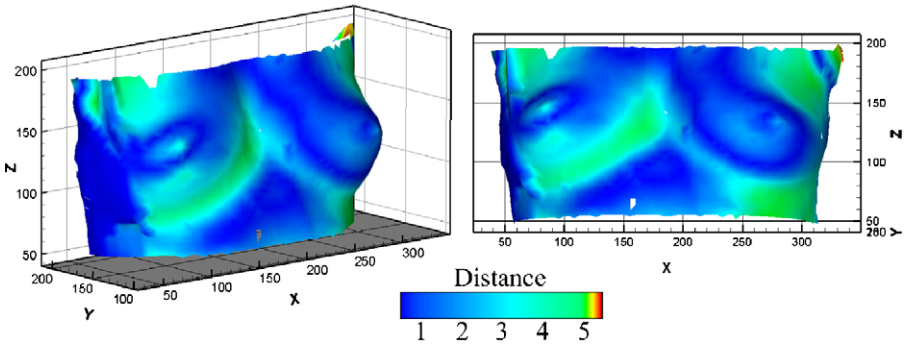

Fig. 10. Displacements undergone by the deformed finite element breast to achieve the actual geometry of Patient B obtained from the 3D scanner data.

patient (captured using a 3D scanner) is superimposed to the deformed mesh of the breast after gravity calculations. This procedure is made modifying the proportion of each tissue, and the qualitative match of the surfaces can be seen. For instance, it can be clearly appreciated that Fig. 8(a) which corresponds to a 40% fat/60% gland breast, fitted much better than Fig. 8(b) in which fat proportion was increased.

To validate the accuracy of the model, an algorithm was implemented to measure the distance between each node on the deformed mesh and its corresponding location on the 3D surface. The coupling of both surfaces can be seen in Fig. 9.

The accuracy of the fitting was computed by means of the distance between the finite element solution and the real surface of the patient in the standing up position. This can be seen in a colour map of the breast as shown in Fig. 10. The mean deviation between both surfaces is 2.4 mm.

4. Discussion

The breast has an inhomogeneous structure containing many layers of different kinds of tissue. However, the two predominant types of tissue within the breast are fat and normal glandular tissue which supports lactation. The proportion of each tissue in a breast depends on the age of the woman, if she is pre-menopausal or post-menopausal and, in general, on the specific patient's constitution.

The deformation of soft tissues compromises the accuracy of image-guided surgery based on preoperative images and restricts its applicability. In this paper, we have presented a FE model, based on biomechanical principles, to predict breast tissue deformations, therefore avoiding this limitation. This model could be used as a guideline in numerous clinical applications, such as breast image registration, multimodality data fusion, breast surgery and biopsy. Predicting breast deformations with the reported accuracy would improve the surgical precision for non-palpable lesions, and provide plausible breast deformations for validation and teaching purposes. However, the feasibility of the method depends on a suitable material characterization.

In this study we propose a method to predict deformations of the breast for helping in presurgical planning. Two different tools were used to evaluate the accuracy of the models, the first one consisted of the validation of the position using landmarks and the second in the registration of the patient in standing position comparing the resultant image with the finite element results. These techniques were applied to two different breast models, the first one with a high proportion of fat tissue and the second one with a lower proportion of this tissue. The deformed shape of both breasts was fitted by adjusting the material properties. For simplicity, only an average value of the material properties of fat and gland was introduced taking into account the proportion of each tissue across the data sets. The main result obtained in this work was that the best fit for the material properties that adjusted the final shape of the first data set in standing position, also adjusted the shape for the second data set. We observed that introducing a simple Neo–Hookean model for fat and gland with an estimated value for the coefficient C of 3 kPa and 12 kPa, respectively, was enough to accurately predict the undergone deformation of the breast. These values are in agreement with those obtained by other authors [10,11,14]. Thus, in this work, a very simple method is proposed in order to predict the deformations of the breast when modifying its position. Two different datasets were adjusted using the same material properties only varying the fat/gland proportion as computed from the CT image. In addition, the reconstruction of the real shape of the breast using a 3D scanner gives more information than using landmarks [16] and can be used as an additional tool for the plastic surgeon to construct an anthropometric study. In this paper, the material parameters were adjusted using the data of a young woman and then were applied to simulate the breast deformation of an older woman with a different percentage of fat and gland.

It is clear that a more accurate but less standard model could be constructed using different material properties for gland and tissue distinguishing both volumes. In this paper, a fastest way to assist the surgeon to plan an intervention was sought. In addition, Azar et al. [2] found that a model with very simplified material properties would not significantly affect the results for a given patient. Although, incorporating other important structures such as the Cooper's ligaments or the effect of the pectoral muscle would also improve the accuracy of the model [5], it would involve a loss in simplicity.

To conclude, we were interested in finding the best way of presurgically estimating the morphological modifications of the breast depending on a specific intervention (reduction or augmentation) to perform. This study has demonstrated the ability to predict the deformations of a normal breast depending on the patient posture. These data may be of interest in studies in which the deformation of the breast tissue is analyzed during an augmentation or reduction intervention.

Acknowledgment

The authors gratefully acknowledge the research support from the Spanish Ministry of Science and Technology through the research project FIS2005-0520-C03-03.

References

[1] Azar FS, Metaxas DN, Schnall MD. A deformable finite element model of the breast for predicting mechanical deformations under external perturbations. Acad Radiol 2001;8:965–75.
[2] Azar FS, Metaxas DN, Schnall MD. Methods for modelling and predicting mechanical deformations of the breast under external perturbations. Med Image Anal 2002;6:1–27.
[3] Azar FS. A deformable finite element model of the breast for predicting mechanical deformations under external perturbations. PhD Thesis, University of Pennsylvania; 2001.
[4] Bakic PR. Breast tissue description and modeling in mammography. PhD Thesis, Lehigh University; 2000.
[5] Gambarotta L, Massabo R, Morbiducci R, Raposio E, Santi P. In vivo experimental testing and model identification of human scalp skin. J Biomech 2005;38:2237–47.
[6] Hibbit and Karlsson and Sorensen, Inc. Abaqus user's manual, v. 6.2. Pawtucket, RI, USA: HKS inc.; 2001.
[7] Krouskop TA, Wheeler TM, Kallel F, Garra BS, Hall T. The elastic moduli of breast prostate tissues under compression. Ultrason imaging 1998;20:151–9.
[9] Reishner R, Balogh B, Menzel E. Two dimensional elastic properties of human skin in temrs of an incremental model at the in vivo configuration. Med Eng Phys 1995;17(4):304–13.
[10] Roose L, Maerteleire W, Mollemans W, Suetens P. Validation of different soft tissue simulation methods of breast augmentation. Int Congr Ser 2005;1281:485–90.
[11] Poplack SP, Paulsen KD, Hartov A, Meaney PM, Pogue BW, Tosteson TD, et al. Electromagnetic breast imaging: average tissue property values in women with negative clinical findings. Radiology 2004;231:571–80.
[12] Ruiter N, Muller T, Stotzka R, Gemmeke H, Reichenbach J, Kaiser W. Automatic image matching for breast cancer diagnostics by a 3D deformation of the mamma. Biomed Tech 2002;47:644–7.
[13] Samani A, Bishop J, Yaffe MJ, Plewes DB. Biomechanical 3-D finite element modelling of the human breast using MRI data. IEEE Trans Med Imaging 2001;20:271–9.
[14] Samani A, Plewes D. A method to measure the hyperelastic parameters of ex vivo breast tissue samples. Phys Med Biol 2004;49:4395–405.
[15] Schnabel JA, Tanner C, Castellano-Smith AD, Degenhard A, Leach MO, Hose DR, et al. Validation of nonrigid image registration using

finite-element methods: application to breast MR images. IEEE Trans Med Imaging 2003;22:238–47.
[16] Tanner C, Schanabel JA, Hill DLG, Hawkes DJ. Factors influencing the accuracy of biomechanical breast models. Med Phys 2006;33(6):1758–69.
[17] Washington CW, Miga MI. Modelity independent elastography (MIE): a new approach to elasticity imaging. IEEE Trans Med Imaging 2004;23:1117–28.
[18] Wellman PS. Tactile imaging. PhD Thesis, Harvard University; 1999.